



An Innovative Way of Utilizing Wave Energy to Counteract Eutrophication and Hypoxia

Margheritini, Lucia; Claeson, Lennart

Published in:
9th ewtec 2011

Publication date:
2011

Document Version
Publisher's PDF, also known as Version of record

[Link to publication from Aalborg University](#)

Citation for published version (APA):
Margheritini, L., & Claeson, L. (2011). An Innovative Way of Utilizing Wave Energy to Counteract Eutrophication and Hypoxia. In A. S. Bahaj (Ed.), *9th ewtec 2011: Proceedings of the 9th European Wave and Tidal Conference, Southampton, UK, 5th-9th September 2011* University of Southampton.

General rights

Copyright and moral rights for the publications made accessible in the public portal are retained by the authors and/or other copyright owners and it is a condition of accessing publications that users recognise and abide by the legal requirements associated with these rights.

- Users may download and print one copy of any publication from the public portal for the purpose of private study or research.
- You may not further distribute the material or use it for any profit-making activity or commercial gain
- You may freely distribute the URL identifying the publication in the public portal -

Take down policy

If you believe that this document breaches copyright please contact us at vbn@aub.aau.dk providing details, and we will remove access to the work immediately and investigate your claim.

An Innovative Way of Utilizing Wave Energy to Counteract Eutrophication and Hypoxia

Lucia Margheritini¹, Lennart Claeson²

¹*Department of Civil Engineering, Aalborg University
Sohngaardsholmsvej 57-9000 Aalborg, DK*

¹lm@civil.aau.dk

²*IVL Swedish Environmental Research Institute Ltd.
P.O. Box 21060 - 100 31 Stockholm, SE*

²lennartclaeson@tele2.se

One of the most urgent environmental issues in 415 coastal systems worldwide is eutrophication and hypoxia [1]. Cause of eutrophication is the rapid increase in intensive agricultural practices, industrial activities, and population growth which together have increased nitrogen and phosphorus flows in the environment. This is a major problem in the Baltic Sea. The present study introduces the Wave-Energized Baltic Aeration Pump (WEBAP). This is one floating overtopping device that uses the collected overtopping water to oxygenate the sea bottom in areas suffering from eutrophication. This is done by using the driving head of the overtopping water temporarily stored in the reservoir flowing out through a long vertical pipe leading close to the bottom of the sea. The necessary amounts of oxygen and corresponding overtopping volumes in order to have a positive impact in a damaged environment have been considered for the Baltic Sea case and laboratory tests in scale 1:25 to the North Sea have been conducted in the 3D deep wave basin at the Hydraulics and Coastal Engineering Laboratories of Aalborg University. The ‘prove the concept’ and investigation of motions forces are here presented with focus on extreme wave conditions providing relevant insight on technical aspects.

Overtopping. Oxygenation. Eutrophication. Moring Forces. Multipurpose Platforms. Motion Transfer Function.

I. INTRODUCTION

Patents from wave energy machines date back at least to the middle of the 1800 a.C.. At that time wave energy uses other than electricity production were also considered. For example, the “Santa Cruz Wave Motor” [2] was designed to pump up to a higher level the water from the sea and use it to spray and wash a close by railway. In a similar way, the Wave-Energized Baltic Aeration Pump (WEBAP) has been conceived in order to pump oxygenated water to the bottom of the sea, more than 80 m below the mean sea level. The Baltic Sea’s surface area is 415 000km² and the average depth is only 60 m. The catchment is large, 1 641 650km² (Fig.1) and river runoff of fresh water is significant compared to the restricted exchange of saline sea water through the shallow (17 m) Danish straits (Fig. 1). Large intrusions of saline water are dependent on special weather conditions and do not occur regularly, or even annually. All conditions give rise to a stable stratification of the water body, with a halocline at 60-80 m depth and a salinity gradient from north to south. The strong

stratification together with decreasing salt water intrusions has lead to a situation with severe oxygen deficits in many deep-water areas in the Baltic Sea. The internal vertical mixing of fresh oxygen-rich surface water and deep water is hindered by the stratification, and new oxygen-rich water with high salinity has not entered the basin during recent years. When excess of nutrients (nitrogen and phosphorus) produced by the increased human activities reach the coastal systems, then they can cause excessive growth of phytoplankton, microalgae (e.g., epiphytes and microphytes), and macroalgae (i.e., seaweed). These, sequentially, can lead to other losses of biodiversity, damage of coral reef damage and low dissolved oxygen.

The Baltic Sea is affected by eutrophication to a significant degree. For several decades the inflow of nutrients has been higher than background levels and nutrient concentration levels have increased considerably during the last century. Excessive blooms of cyanobacteria have occurred during summers of many of the latest years covering large parts of the Baltic Proper. Anoxia has spread and now covers a bottom area of around 100 000 km² [3]. Increasing levels of chlorophyll and summer phytoplankton has been observed [4], as well as decreased water transparency. Lower catches and collapses of top-consumers such as cod are also a present threat, at least partly caused by eutrophication. These species have also been subject to heavy fishing which strongly contributes to the pressing situation today. In addition the flat-fish stock is threatened by eutrophication.

The idea to use floating breakwaters to oxygenate the anoxic bottoms and the deep water of the Baltic Sea originates in this form from an independent non-profit organization called O2-gruppen [5], WavePlane [6] and WaveDragon thought about oxygenation as a complementary function of their wave energy turbine. Finally, another proposal to counteract the oxygen depleting situation and the excessive algal blooms in the Baltic Sea is the “halocline ventilation by mid-water mixing” [7]. In the overall, previous to this work, specific technical aspects have not been discussed, but mainly the conceptual mitigating ideas and their possible outcomes have been considered.

Three wave gauges (sample frequency: 25 Hz) have been installed in front of the system to measure incident and reflected waves, generated by software AwaSys 5. The model has been equipped with:

- No. 2 load cells on the mooring lines, sample frequency: 25 Hz.
- No. 1 MTi to measure the movement of the body under waves excitation i.e. roll, pitch and yaw, as well as accelerations in the three directions, sample frequency 25 Hz (A appendix).
- No. 1 propeller to measure rotational speed proportional to flow velocity inside the pipe.
- No. 2 small wave gauges in the reservoir to measure the water level.

The device was tested under 2D irregular waves (Jonswap spectrum 3.3) for the conditions in Table 1 supplied by the developer. Length of each test is 30 minutes. $T_p=1.4 T_z$ has been used. A total of 18 tests with two different mooring stiffnesses S1 and S2 have been conducted. The influence of the buoyancy level has also been investigated. The data acquisition has been handled by WaveLab3. The same software allowed also the analysis of the mooring forces, generated waves and water levels inside the reservoir. The propeller revolutions were noted down at regular intervals of time during the tests. The movement data were handled by the MTi software in a different computer. Outputs were: pitch, roll, yaw and accelerations in the three reference directions. The movements' analysis has been carried out with a Matlab routine. Indeed, the Mti instrument acquires pitch, roll, yaw and the accelerations in the three dimensions. The last ones needed to be double integrated to obtain the displacements.

TABLE 1. INPUT WAVES USED AND CORRESPONDING FULL SCALE.

	PM spectrum 1:25		PM spectrum 1:1	
	Hs [m]	Tz [s]	Hs [m]	Tz [s]
W1	0,024	0,6	0,6	3
W2	0,04	0,72	1,0	3,6
W3	0,096	1,02	2,4	5,1
W4	0,192	1,38	4,8	6,9

A. Estimation of pipe capacity

Differences in water column density and losses due to the length of the pipe must be won by the driving head in order to have the pump mechanism working. It has been calculated [8] that the minimum head necessary is 0.13 m for a 70 m long pipe, 0.19 m for an 80 m long pipe while only 0.04 m are needed for a 50 m long pipe consider salinity and temperature gradients in the Baltic Sea. This indicates also the water level that will stay permanently in the reservoir. In the laboratory, the pipe was realized with a flexible plastic tube kept vertical by weights attached to the bottom side. Directly scaling the pipe dimensions with Froude law would be imprecise as the flow process is not dominated by gravity forces (as in wave's processes) but by viscous forces that would require a different scaling law (not Froude but Reynolds). Moreover, it is

difficult to scale down properly the roughness of the material when going to the laboratory. Finally, in the laboratory there is no salinity or temperature gradient. It is said that scaling down directly the dimensions of the pipe ($L=70$ m and $D=2.05$ m) with Froude law would give pipe dimensions that would allow a smaller flow; this as result of scaling limitations. Keeping this in mind, the final pipe used in the model is 1.7 m long, has a diameter of 0.10 m and a roughness $k=0.003$. This guarantees flow rates comparable to the ones desired for the full scale. The pipe capacity is plotted in Fig. 4, together with other pipes taken into consideration for the laboratory model.

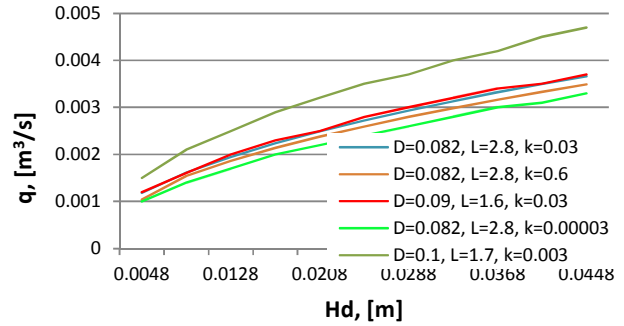


Fig. 4. Different pipe capacities for the laboratory model. D = diameter of the pipe, L = pipe length, k = roughness.

B. Results and Analysis

Mooring forces are presented in terms of statistical peak force parameters conforming to the Rayleigh distribution F1/250 obtained from Wavelab time series analysis of the signal measured by load cells on the mooring lines. The characteristic of the two tested stiffnesses are in Fig. 5. The stiffness is then the inclination of the curves.

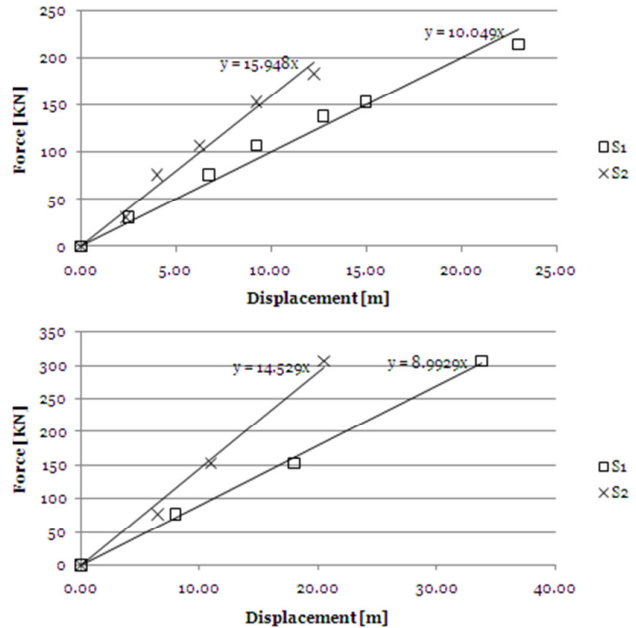


Fig. 5. Tested stiffnesses Front (Top) and Rear (bottom) lines, full scale.

1) *Free oscillation tests.* The free oscillation tests are performed in order to find the natural frequency of the floating body which characterized its shape and hydrodynamic behaviour. For the free oscillation tests, the stiffness S1 was used. The results show a natural frequency of 2.5 seconds for surge, 20 seconds for heave and 2.8 seconds for the pitch (Fig. 6).

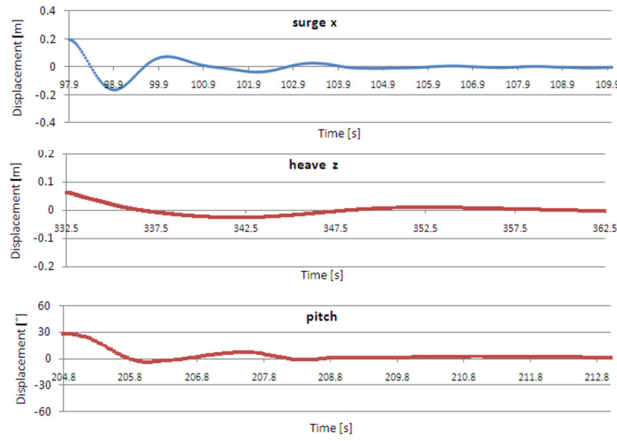


Fig. 6. Free oscillation tests results.

For the surge it has been noticed that when the structure was let free after it was pulled from the rear mooring, while the device was smoothly moving backward, it was getting stuck moving forward due to the extension of the front ramp. This can be noticed in seconds 99.9-101.9 where the device is moving forward. The device is moving forward also between seconds 97.9 and 98.9 but the dragging force of the mooring recalling the device forward is stronger than the friction generated by the ramp as the device has just been released after the rear mooring has been pulled.

For the heave, a quite long natural frequency was found. This could be justified by the presence of the pipe.

The pitch is almost independent of the mooring system. We can notice that device tilts easier forward than backwards, generating bigger displacements on the positive side of the Y axis. Indeed, the oscillations on the positive side of the Y axis represent the tilting of the front, while the tilting of the back results blocked by the presence of the pipe which is in the rear side of the structure.

2) *Mooring forces.* Forces are here presented in full scale through the key statistical parameter $F1/250$ and without the pretension. The maximum $F1/250$ obtained is on the front mooring for the S2 and draft of 0.55 m below sea water level, under $Hm0=4.22$ m. This force corresponds to $F1/250=102.9$ KN. The second highest force is $F1/250=89.5$ KN and occurs mooring stiffness S1 with a draft again of 0.55 m and Hm_0 4.19 m. Further results are presented and extrapolated in Fig. 8. Mooring forces increase linearly with the wave height. Higher forces are associated with S2 stiffer configuration, as expected. The average difference on front mooring forces between configurations S1 and S2 is 23.5%.

By lowering the structure and increasing the draft, there is a change on the mooring forces. This can be seen by comparing the curves S2 and S2B2 in Fig. 7. Indeed, by lowering the crest (i.e., increasing the draft) of 0.38 m (passing from $dr1=0.55$ m to $dr2=0.93$ m. B2 test tag) under configuration S2, we recorded a decrease on mooring forces of around 10% on the front line. This is also an expected result as forces on floating bodies, decreases when lowering the structure under mean water level where the amplitude of particles' motion under wave action is smaller and decreases while increasing water depth.

The maximum $F1/250$ obtained on the rear mooring is for the S2 and draft of 0.55 m below sea water level, under $Hm0=4.22$ m. This force corresponds to $F1/250=51.11$ KN. Similar behaviour of the front mooring is recognized for the rear mooring, despite performed tests failed to show results as clearly as for the front mooring. Indeed, the size of the model and perhaps not enough difference on the two chosen stiffnesses resulted in the over-looping of the curves representing the dependency of the rear mooring force on the significant wave height for S1 and S2 (Fig. 8). Nevertheless it is still clear that forces increase with the increasing wave height and that a lower structure (bigger draft) reduces the forces on the mooring line.

In average, the forces on the front mooring are twice as much the ones on the rear mooring that are therefore not negligible even if considerably smaller.

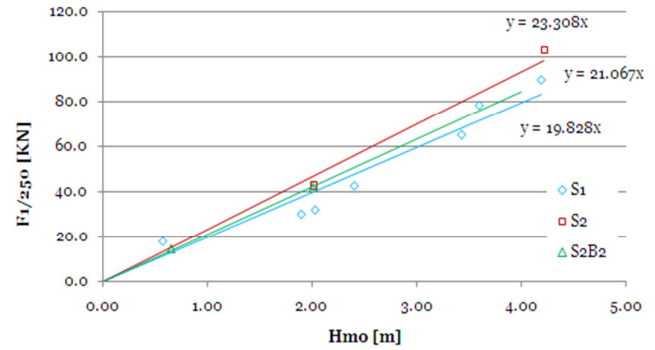


Fig. 7. Dependency of forces on FRONT mooring on $Hm0$, for S1 and S2 and S2B2. Full scale.

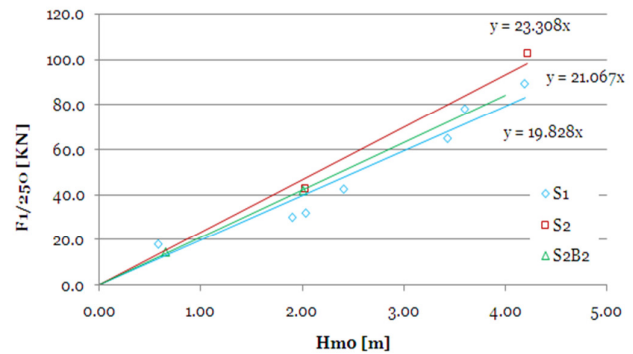


Fig. 8. Dependency of forces on REAR mooring on $Hm0$, for S1 and S2 and S2B2. Full scale.

Finally, the minimum and maximum force distribution for the front line in test W4S2 has been plotted in exponential paper (Fig. 9). This shows a difference of around 40% between the two curves for expedience probabilities higher than 0.5%. Therefore, for bigger waves, it is expected the mooring lines will have to work far away from operating conditions and therefore need to be carefully designed.

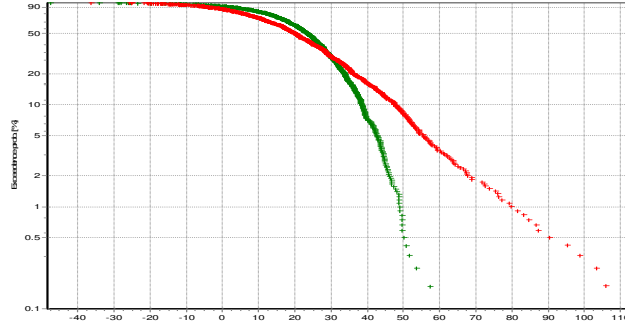


Fig. 9. Force distribution distribution Min (green) and Max (red) in KN, front mooring, $H_{m0} = 4.22$ m and S2.

3) *Motion transfer function.* The motion response of the structure is reported for surge, heave and pitch. We here compare the input (waves' spectral density) to the response (movements' spectral density) to obtain the motion transfer function as the ratio between these two. This is done for two different wave conditions in order to cover a wider range of frequencies. The selected wave conditions for this procedure are the ones obtained by the tests: W4S1 and W3S1 (Fig. 10).

For surge we can see a huge natural response (Fig. 11, top). Indeed, while all the wave energy is concentrated around 0.6-0.9 Hz, the peak response is instead around 0.4-0.5 Hz. This is confirmed by the fact that the natural oscillation for surge was found to be 2.5 s, (frequency=1/T). The transfer function (Fig 11, bottom) for values lower than 0.6 Hz has not been reported as subject to height uncertainties. Indeed, being the transfer function the ratio between the response spectrum and the wave energy spectrum, the result features very high values being the energy input very small. Instead, it is clear that under the influence of waves, the motion is dominated by the moorings.

For heave, the natural response is concentrated at very low frequencies (Fig. 12, top). This is the case because the free oscillations have been found to have a very long period. A small response is also recorded under the action of the incoming waves, around 0.6 Hz close to the peak wave period. Also in this case, the transfer function is reliable only for values of Hz bigger than 0.4 (Fig. 12 bottom).

For pitch, we have a response that matches very well the energy input (Fig. 13, top). Indeed the response is concentrated between 0.5 and 1.4 Hz. As for the previous two transfer functions, also here and for the same reasons, the reliable transfer function must be considered for $Hz > 0.5$ (Fig 13, bottom).

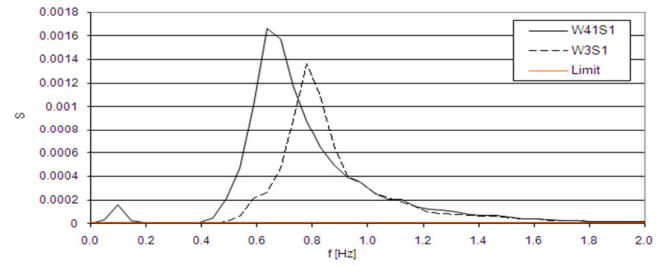


Fig. 10. Input disturbance, (waves' spectral density).

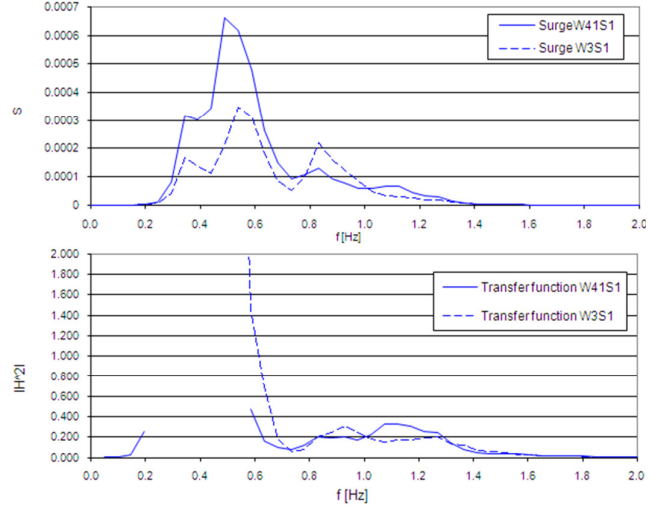


Fig. 11. Response and transfer function for Surge.

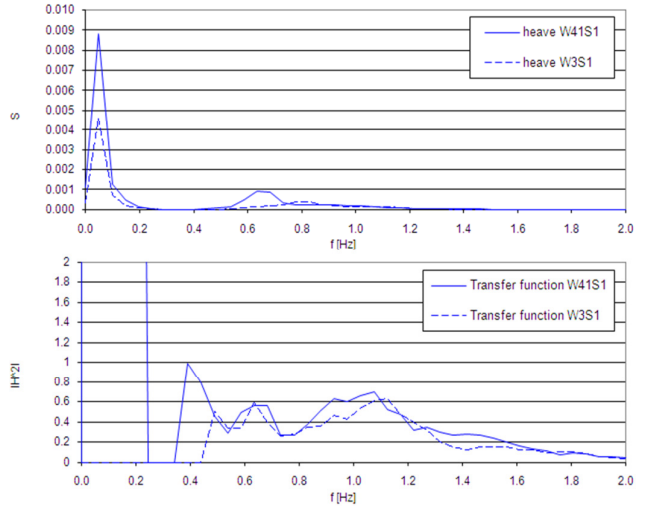


Fig. 12. Response and transfer function for Heave.

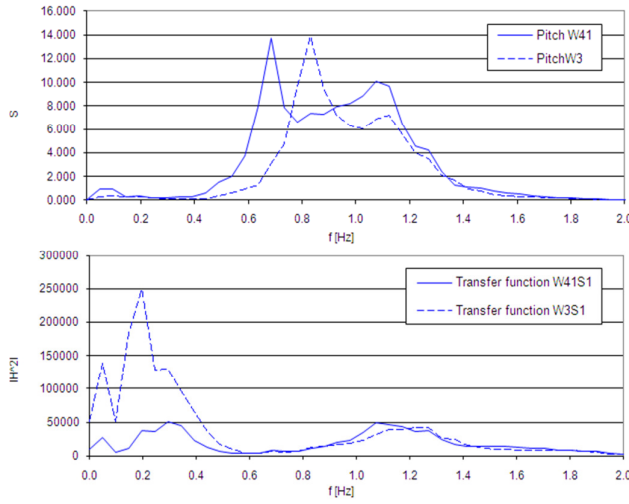


Fig. 13. Response and transfer function for Pitch.

4) *Proof of concept and propeller measurements.* A propeller was installed at the entrance of the pipe at approximately 0.06 m from the entrance (1.5 m real scale). From this point we have measurements of number of revolutions per second (RPS). The number of revolutions is directly proportional to the overtopping flow rate over the crest. Therefore conclusions are made based on this parameter. No overtopping occurred for low sea states (W1 and W2) corresponding to $H_{m0}=0.6$ m real scale in the floating configuration for $R_{c1}=0.7$ m; indeed RPS is equal to zero.

When using a lower crest level $R_{c2}=0.32$ m we can see some overtopping for W2 but still no overtopping for W1. This is to be attributed to the influence of the movements of the device riding the incoming waves. In our case, no significant difference among the different floating configurations has been found, despite the stiffer mooring did prevent a bit the movements (Fig. 14). No significant difference for S1 and S2 and S2B2 is recorded, but it is unlikely that a situation with a stiffer mooring would result in a lower overtopping, keeping all the other conditions the same. Instead, influence of the movements of the floating body on the overtopping can be better noticed when fixing the device (tests' tag: _Fixed_).

It is clear that when the device is fixed instead of floating, bigger volumes of water enter then the reservoir. Indeed, overtopping does occur for W1 and W2 but most of all the overtopping increases of 38% for W3 and 53% for W2 when comparing the fixed configuration to the floating configuration with the same crest level (green and purple test lines in Fig.14).

From the recordings of the 2 small wave gauges inside the reservoir it emerged that the water did never spilled out of the reservoir, not even with higher wave conditions, testifying that the pump mechanism is working properly and pump capacity was sufficient to handle overtopping flow. Standing waves across the reservoir have been noticed as a constant in all tests.

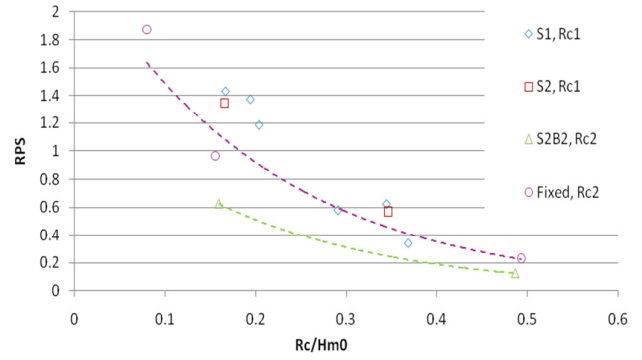


Fig. 14. Dependency of the RPS on H_{m0} for different configurations.

IV. OVERTOPPING CALCULATIONS

Stigebrandt and Gustafsson [7] suggest that 100 kg of O_2 per second, which would correspond to 3.1×10^6 ton/year, would have to be added to subhalocline waters in the whole Baltic Sea to obtained the desired results, i.e. to keep the waters well oxygenated, and thereby reduce P concentrations, in a fairly short period of time. The conclusion from Zillén and Conley [9] is also that 63-190 kg/s of O_2 is the required theoretical oxygen supply. The floating structure under exam is a low crested structure, very similar to WaveDragon (Fig. 15).

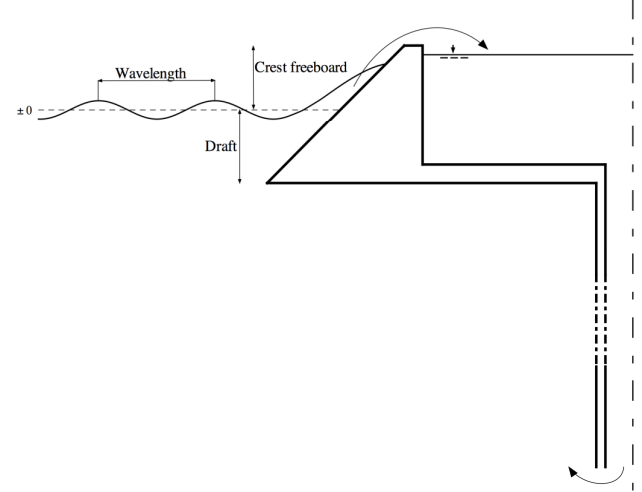


Fig. 15. WEBAP working principle.

It is then possible to calculate the overtopping flow with sufficient accuracy using the formulation by Kofoed [10]:

$$\frac{q}{\lambda_m \lambda_a \lambda_{dr} \lambda_s \sqrt{g H_s^3}} = 0.2 e^{-2.6 \frac{R_c}{H_s} \frac{1}{\gamma_r \gamma_b \gamma_h \gamma_\beta}} \quad (1)$$

Where H_s is the significant wave high, R_c is the crest free board and g the gravity acceleration $= 9.81 \text{ m/s}^2$. The λ factors take into account different geometrical parameters such as varying slope angle, draft extension (dr) and small dimensionless free board $R=R_c/H_s$. The γ coefficients are reduction coefficients as defined by van der Meer and Janssen

[11]. By mean of the above equation, the influence of different parameters such as crest free board R_c , draft extension d_r and slope angle α on the overtopping flow rates has been explained.

A. Crest free board

For a fixed geometry and a slope angle of 23° , different crest freeboards are obtained by changing the buoyancy level of the model, meaning that when we increase the R_c (crest free board) we decrease d_r (draft), therefore the sum $R_c + d_r$ is a constant = 1.25 m in full scale. Therefore, in the present calculations R_c and d_r are not independent one from the other. Based on this assumption, the results the overtopping discharge has been calculated in four different wave conditions Fig 16.

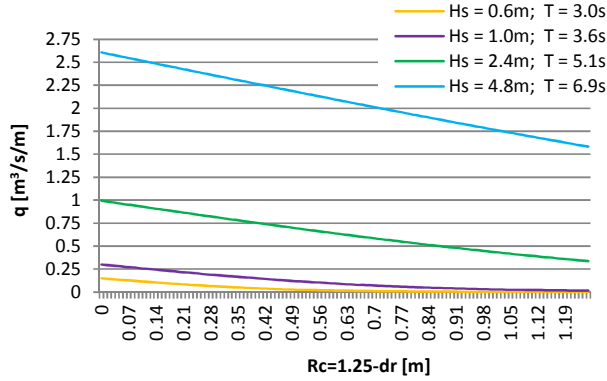


Fig. 16. Dependency of the overtopping discharge on the R_c and d_r , for different wave conditions. Full scale values, geometry based on configuration with solid draft, slope angle $=23^\circ$.

B. Ramp Extension

Extending the front ramp increases the draft of the floating body and the overtopping volumes by directing the flow that would pass under the device, to the reservoir. Based on this idea, the developer expressed the wish of adding a stretched cloth fixed on a steel frame to make the ramp longer and “capture” that flow. Despite the cloth not being the optimal solution to reach the purpose, calculations with three different “ramp extensions” have been made, in order to show what is possible to gain with such an implementation. The calculations, are instead based on Equation (1) and therefore on one geometry where the ramp extension makes up one piece with the entire structure. In the equation used to calculate the average overtopping discharge, the ramp extension is expressed by the coefficient λ_{dr} and therefore by the draft:

$$\lambda_{dr} = 1 - k \frac{\sinh\left(2k_p d\left(1 - \frac{d_r}{d}\right)\right) + 2k_p d\left(1 - \frac{d_r}{d}\right)}{\sinh(2k_p d) + 2k_p d} \quad (2)$$

where k_p is the wave number based on L_p = wave length based on T_p and k is a coefficient controlling the degree of influence of the limited draft. k is found to be 0.4 by best fit to Kofoed [10] tests; d is the water depth and the other parameters have been previously described. The expression

taking the dependency of the draft into account is based on the ratio between the time averaged amount of energy flux integrated from the draft up to the surface $E_{f,dr}$ and the time averaged amount of energy flux integrated from the seabed up to the surface $E_{f,d}$ (Fig. 17):

$$\frac{E_{f,dr}}{E_{f,d}} = 1 - \frac{\sinh\left(2k_p d\left(1 - \frac{d_r}{d}\right)\right) + 2k_p d\left(1 - \frac{d_r}{d}\right)}{\sinh(2k_p d) + 2k_p d} \quad (3)$$

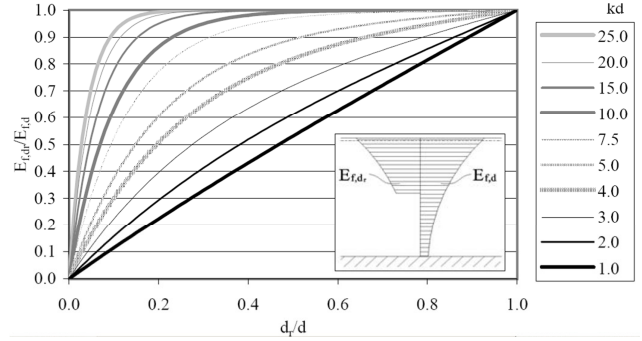


Fig. 17. The ratio in Eq. 3 as a function of the relative draft for various values of kd .

In the derivation of Eq. 3 linear wave theory is used. Because of the limitations of the linear wave theory Eq. 3 cannot completely describe the effect of limited draft on overtopping. Using λ_{dr} equal to Eq. 3 would lead to an estimation of zero overtopping for $d_r=0$ which obviously is not the case for all combinations of H_s and R_c . Therefore the coefficient $k=0.4$ is introduced and the expression for λ_{dr} given in Eq. 2 is obtained.

For the selected geometry with slope angle of 23° , overtopping calculations have been made for a ramp extension of 2 m, 4 m and 6 m varying separately the draft d_r and the crest level R_c that are not longer considered dependent on each others. However, if the WEBAP structure will be realized with a flexible slope, the results that follow must be decreased proportionally to the weakness of the material used. The losses depend on details that are not known at the present time of development of the device, such as the material of the extension, the connection to the main body, the inclination angle. It would be indeed expected that a flexible material without a rear support, would block and direct only a negligible flow to the reservoir, while most of it would pass under the structure. In addition such a solution may be not resistant and durable.

Extending the ramp has positive effects on maximization of the overtopping volumes (Fig. 18-21). In average, we foreseen an increase of overtopping volumes up to 16.5% for a ramp extension of 2 m compared with the case with no ramp extension for $H_s = 0.6$ m while for waves with $H_s = 4.8$ m the increase in overtopping is 6.9 %, with smaller variance compared to the case with smaller waves. This is because for smaller waves the overtopping is zero until the R_c is roughly 0.55 m and $d_r=0.70$ m, being the waves too small to overtop the crest. Therefore an increase in the draft is more effective

for lower sea states than in bigger waves as most of the incoming waves would overtop the crest anyways.

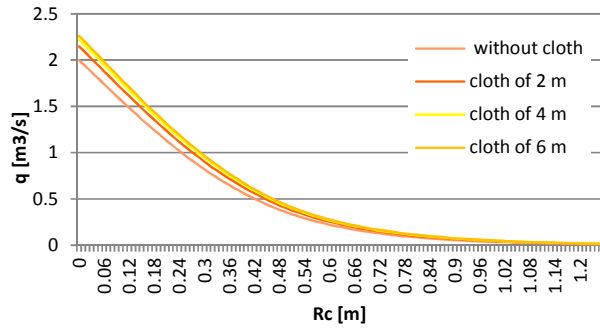


Fig. 18. Overtopping for different ramp's lengths; $H_s=0.6\text{ m}$, $T=3\text{ s}$, device length = 13.5 m.

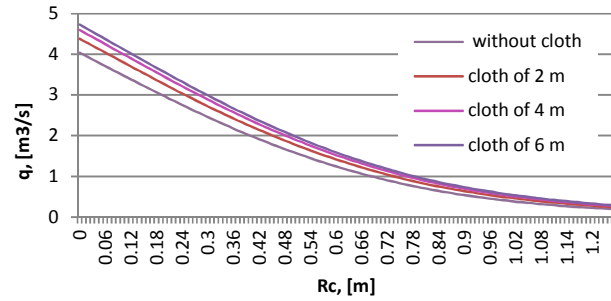


Fig. 19. Overtopping for different ramp's lengths; $H_s=1.0\text{ m}$, $T=3.6\text{ s}$, device length = 13.5 m.

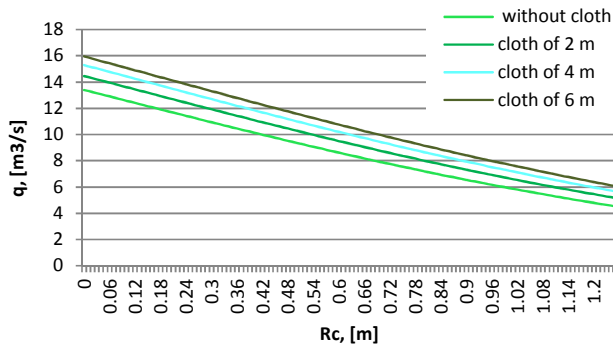


Fig. 20. Overtopping for different ramp's lengths; $H_s=2.4\text{ m}$, $T=5.1\text{ s}$, device length = 13.5 m.

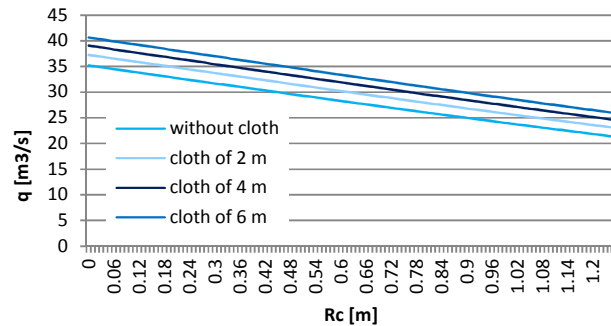


Fig. 21. Overtopping for different ramp's lengths; $H_s=4.8\text{ m}$, $T=6.9\text{ s}$, device length = 13.5 m.

With 2 m ramp extension, 0.020 m³/s/m of overtopping flow rates are reachable with $R_c = 0.58\text{ m}$ while without the ramp the same results needs $R_c = 0.55\text{ m}$. If the ramp extension is 6 m, then an average increase on the overtopping flow rate of 29% is expected for $H_s = 0.6\text{ m}$ while an increase of 13% in the case with $H_s=4.8\text{ m}$.

For an $R_c = 1.25\text{ m}$ (Table 1) and $H_s = 0.6\text{ m}$ a ramp extension of 2 m with slope inclination of 23° , corresponding to a draft of 0.8 m, would generate an overtopping flow rate of 0.0010 m³/s/m; compared to the case with no draft that gives 0.0008 m³/s/m we have an increase of 33%. For $H_s = 1.0\text{ m}$ passing from 2 m to 6 m a ramp extension would increase the overtopping flow rates from 0.0178 m³/s/m to 0.0214 m³/s/m corresponding to an increase of 25% and 51% respectively compared with the case with no draft that have an overtopping of 0.0142 m³/s/m. For $H_s=2.4\text{ m}$ the increase in overtopping passing from the case with no ramp and the case with 6 m long ramp foreseen an increased in overtopping of 34% going from 0.3360 m³/s/m to 0.4503 m³/s/m while for $H_s=4.8\text{ m}$ gives an increase of 21% with the longest extension.

TABLE 2. OVERTOPPING FLOW RATES [M³/S/M] IN DIFFERENT WAVE CONDITIONS FOR $R_c=1.25\text{ m}$ AND VARYING CLOTH LENGTH.

dr [m]	0,0	2 m length = 0,8 draft	4 m length = 1,5 m draft	6 m length = 2,3 m draft
$H_s=0.6\text{ m}$, $R_c=1.25\text{ m}$	0,0008	0,0010	0,0011	0,0012
$H_s=1.0\text{ m}$, $R_c=1.25\text{ m}$	0,0142	0,0178	0,0200	0,0214
$H_s=2.4\text{ m}$, $R_c=1.25\text{ m}$	0,3360	0,3834	0,4208	0,4503
$H_s=4.8\text{ m}$, $R_c=1.25\text{ m}$	1,5817	1,7103	1,8232	1,9223

Finally the influence of the slope angle is presented. In total four different slope angles have been considered: 23° as suggested by the developer, 15° , 30° and 35° . Trends are similar to the ones presented in Fig. 18-21.

The higher overtopping occurs for angles between 23° and 35° . While graphically there is a noticeable difference for the case featuring 15° and generating the lowest overtopping, almost no difference shows for the remaining cases across all the wave conditions.

V. CONCLUSIONS

A total of 18 tests have been run with WEBAP model in scale 1:25 in different configurations and wave conditions. Previously, free oscillation tests had shown natural frequency for surge corresponding to 2.5 seconds. For heave 20 seconds and 2.8 seconds for pitch.

The maximum generated wave height corresponds to $H_s=4.22\text{ m}$ and $T_p=8.715\text{ s}$. Under the action of these waves, the maximum mooring force occurred. This force is 102.9 kN on the front mooring and 51.11 kN on the rear mooring.

Higher forces correspond to bigger waves and stiffer moorings.

Forces on front mooring are in average twice bigger than forces on the rear mooring.

By lowering the structure, the forces on mooring are reduced. By passing from $dr1=0.55$ and $dr2=0.93$ it is expected a decrease of the mooring force of around 10%.

Movements of the floating body have a negative effect on the overtopping. No overtopping occurs for $H_s=0.6$ m and $H_s=1.0$ m for $R_c1=0.70$ m. The smallest overtopping event recorded was for $R_c2=0.32$ m, draft = 1.43 m and $H_s=0.70$ m. This situation generated RPS in average 10 times smaller than the tests with $H_s \sim 4$ m.

The influence of movements on the overtopping is increasing with H_s . For $H_s=2.4$ m the overtopping decreases of 38% compare to the case of a fix structure with same R_c , while decrease of 53 % for $H_s=4.8$ m.

Transfer functions for surge, heave and pitch have been given. It seems that the first two are dominated by the mooring characteristics. The heave movement is very slow. During the tests it was noticed that the device was riding the waves very much.

ACKNOWLEDGMENT

The author wants to thank Christian Baresel for his collaboration in the project as well as Christoffer Carstens for his Master Thesis work that allowed the problem formulation related to the technical aspects presented in the present article.

REFERENCES

- [1] M. Selman, S. Greenhalgh, R. Diaz and Z. Sugg "Eutrophication and Hypoxia in Coastal Areas: A global Assessment of the State of Knowledge". WRI Policy Note. Water quality: Eutrophication and Hypoxia No1. World Resource Insitute, 2008
- [2] The Santa Cruz Wave Motor website. [Online]. Available: http://www.haskey.com/johnh/wave_motor/index.html.
- [3] E. Bonsdorff, C. Rönnerberg and K. Aarnio, "Some ecological properties in relation to eutrophication in the Baltic Sea". *Hydrobiologia, Kluwer Academic Publishers*. 2002, 475-476:371-377.
- [4] S. Suikkanen, M. Laamanen and M. Huttunen, "Long-term changes in summer phytoplankton communities of the open northern Baltic Sea". *Estuarine, Coastal and Shelf Science*, 2007, 71(3-4):580-592.
- [5] O2-gruppen website. [Online]. Available: www.o2gruppen.se.
- [6] WavePlane website. [Online]. Available: <http://waveplane.com/>.
- [7] A. Stigebrandt and B. G. Gustafsson, "Improvement of Baltic Proper water quality using large-scale ecological engineering". *AMBIO*, 2007, 27(2-3):280-286.
- [8] L. Margheritini, S. Parmeggiani, J.P. Kofoed; A. Sumila, "Proof of concept: Wave Energized Baltic Aeration Pump (WEBAP)", Tech. Rep., Department of Civil Engineering, Aalborg University, *DCE n.82*, 2010.
- [9] L. Zillén and D. J. Conley, "Potential management techniques, environmental effects and ethics Report from the 3rd Baltic Sea 2020 workshop on hypoxia in the Baltic Sea", *BalticSea2020, Tec. Rep.*, 2007.
- [10] J.P. Kofoed, "Wave Overtopping of Marine Structures –Utilization of Wave Energy". Ph.D. Thesis, Aalborg University. Hydraulics & Coastal Engineering Laboratory, Department of Civil Engineering, 2002.
- [11] J.W. Van der Meer and J. P. F. M. Janssen, "wave run up and wave overtopping at dikes". Tech. Rep., Task Committee Reports, *ASCE*, 1995.
- [12]